LA-UR-19-23292
Approved for public release; distribution is unlimited.

Title: Characterization of 14YWT & ODS Base Metals

Author(s): Eftink, Benjamin P.
Lear, Calvin Robert
Lienert, Thomas J
Maloy, Stuart Andrew

Intended for: Report

Issued: 2019-04-12

Disclaimer:
Los Alamos National Laboratory, an affirmative action/equal opportunity employer, is operated by Triad National Security, LLC for the National Nuclear Security Administration of U.S. Department of Energy under contract 89233218CNA000001. By approving this article, the publisher recognizes that the U.S. Government retains nonexclusive, royalty-free license to publish or reproduce the published form of this contribution, or to allow others to do so, for U.S. Government purposes. Los Alamos National Laboratory requests that the publisher identify this article as work performed under the auspices of the U.S. Department of Energy. Los Alamos National Laboratory strongly supports academic freedom and a researcher's right to publish; as an institution, however, the Laboratory does not endorse the viewpoint of a publication or guarantee its technical correctness.

Characterization of 14YWT & ODS Base Metals

Prepared for
U.S. Department of Energy

Benjamin P. Eftink
Calvin R. Lear
Thomas J. Lienert
Stuart A. Maloy
04/05/2019

DISCLAIMER

Los Alamos National Laboratory, an affirmative action/equal opportunity employer, is operated by the TRIAD National Security, LLC for the National Nuclear Security Administration of the U.S. Department of Energy. By approving this article, the publisher recognizes that the U.S. Government retains nonexclusive, royalty-free license to publish or reproduce the published form of this contribution, or to allow others to do so, for U.S. Government purposes. Los Alamos National Laboratory requests that the publisher identify this article as work performed under the auspices of the U.S. Department of Energy. Los Alamos National Laboratory strongly supports academic freedom and a researcher's right to publish; as an institution, however, the Laboratory does not endorse the viewpoint of a publication or guarantee its technical correctness.

SUMMARY

Nanostructured ferritic alloys (NFA) with oxide dispersion strengthening are being developed for next generation reactor applications. Applications such as transmutation of long lived isotopes in used fuels require cladding materials that can withstand high irradiation doses, potentially in the hundreds of displacements per atom (dpa). Currently, however, there are no joining processes that retain the strength and fine distribution of oxide precipitates characteristic of ODS alloys. As part of a larger effort to adapt a solid state capacitive discharge welding technique for use with ODS cladding, presented will be characterization of the initial materials including 14YWT and MA956 ODS alloys.

TABLE OF CONTENTS

SUMMARY iv

1. Introduction 1

2. Materials and Methods 1

3. Results and Discussion 2

4. Conclusions 4

5. References 4

Intentionally Blank

1. Introduction

Cladding materials for Generation IV fast reactors, such as the sodium fast reactor, will be subjected to irradiation damage levels in the hundreds of dpa and temperatures of 400-600 °C, above those required for current generation light water reactors. Ferritic ODS steels such as 14YWT are candidate materials for these service conditions based on their resistance to swelling, high thermal conductivity, and sufficient mechanical properties at high temperature. It is necessary, however, to join ODS steel components before they can be used in nuclear reactors. ODS steels are produced such that a high density of uniformly distributed nano-scale oxide precipitates are in the microstructure. While these nano-oxide precipitates strengthen the material, they may also act as sinks or recombination sites for irradiation induced interstitial and vacancy defects. Fusion welding techniques have been unsuccessful in joining ODS alloys, as the dispersed oxides agglomerate in the melted zone and reduce material strength. Solid state welding techniques are thought to be more suitable for ODS alloys, as the material is not melted during welding [1].

2. Materials and Methods

2.1 Materials

Two alloys, 14YWT and MA956, were acquired in tube form with a ~10 mm outer diameter and ~0.5 mm wall thickness. Compositions are given in Table 1 for both alloys. The 14YWT alloy was pilgered at CEA using four 40 % reductions at room temperature, with intermediate anneals at 1200 °C. The MA956 was extruded over a mandrel at room temperature, with intermediate hydrogen anneals at 1000 °C.

Table 1: Compositions of alloys in weight %.

Alloy ID	Fe	Cr	Y	W	Ti	O	C	Mn	Al	Cu	Ni
14YWT	bal	14.4	0.21	3.10	0.39	0.116	0.016	-	0.025	-	-
MA956	bal	19.4	0.85	-	0.42	-	0.020	0.10	4.21	0.074	0.057

2.2 Electron microscopy characterization

Samples were prepared for electron backscatter diffraction (EBSD) by mechanical polishing, with a final step of 0.04 µm colloidal silica. EBSD was performed using a FEI Apreo scanning electron microscope (SEM) using an EDAX detector using TSL software. Scanning transmission electron microscopy (STEM) was performed on a FEI Tecnai F30 operating at 300 keV. Samples were prepared for STEM by focused ion beam (FIB) milling using a FEI Helios 600i. FIB sample preparation started at 30 kV, and the voltage was reduced to 2 kV for final polishing to reduce sample preparation artifacts.

3. Results and Discussion

3.1. EBSD Characterization

The ODS tubes were sectioned and mounted for EBSD such that the transverse and longitudinal cross-sections could be observed. Figure 1 shows a sectioned sample, with "A" defining the transverse cross-section and "B" defining the longitudinal cross-section.

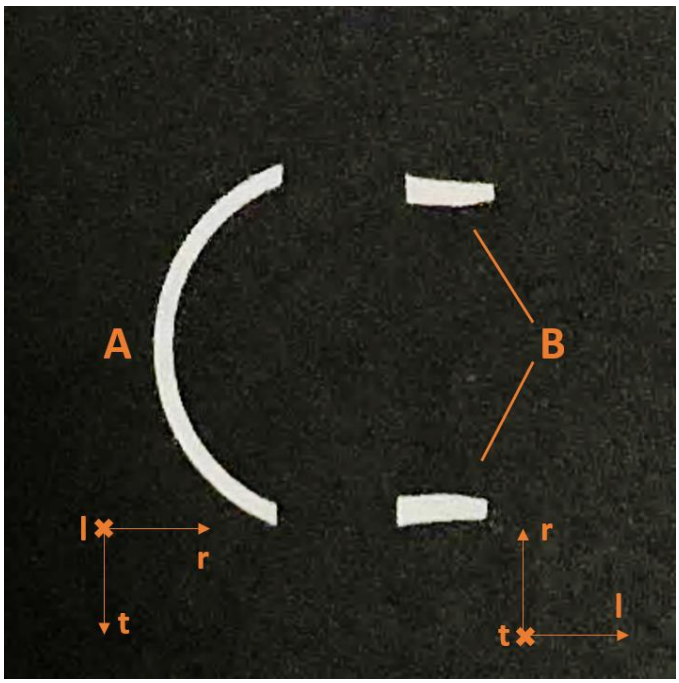

Fig. 1: Optical micrograph of sectioned tube. "A" allows EBSD mapping of the transverse cross-section, while "B" allows EBSD mapping of the longitudinal direction.

The 14YWT sample had grains on the order of 10-50 µm in the smallest dimension and were elongated along the longitudinal direction. Figure 2 shows EBSD orientation mapping in both the (a) transverse and (b) longitudinal direction. Also apparent in the EBSD orientation maps is the contrast within the grains, suggesting dislocation content within the grains.

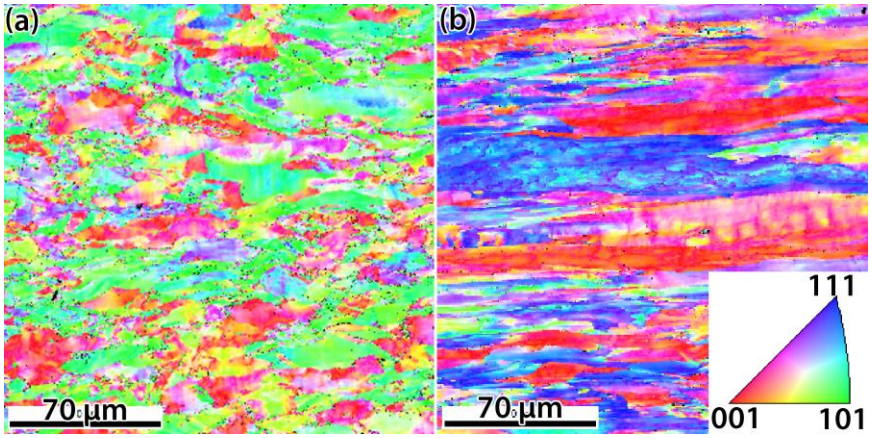

Fig. 2: EBSD orientation mapping of 14YWT tube in the (a) transverse and (b) longitudinal direction.

The MA956 sample by comparison had much larger grains than the 14YWT material, as shown in the orientation maps in Fig. 3. In the smallest dimension the grains are observed to be on the order of 200 µm, an order of magnitude larger than those in 14YWT. While the grains were elongated in the longitudinal direction as before, they were also elongated in the transverse direction. Orientation maps shown in Fig. 3 also reveal sub-grain features, indicating dislocation content within the grains.

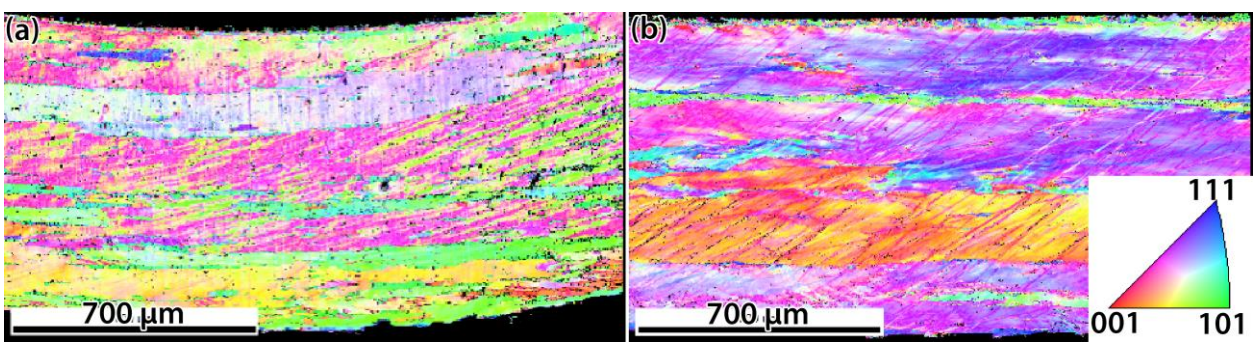

Fig. 3: EBSD orientation mapping of MA956 tube in the (a) transverse and (b) longitudinal direction.

3.2 TEM Characterization

Characterization of the microstructures using TEM is shown in Figs. 4 and 5 for 14YWT and MA956, respectively. In the HAADF image in Fig. 4, the oxide precipitates in 14YWT appear darker in the image and are marked using arrowheads. The average diameter of the oxides is 5 nm with a standard deviation of 2.7 nm. The spatial distribution of the oxide precipitates is generally uniform throughout the TEM sample, although some clustering is observed at grain and subgrain boundaries.

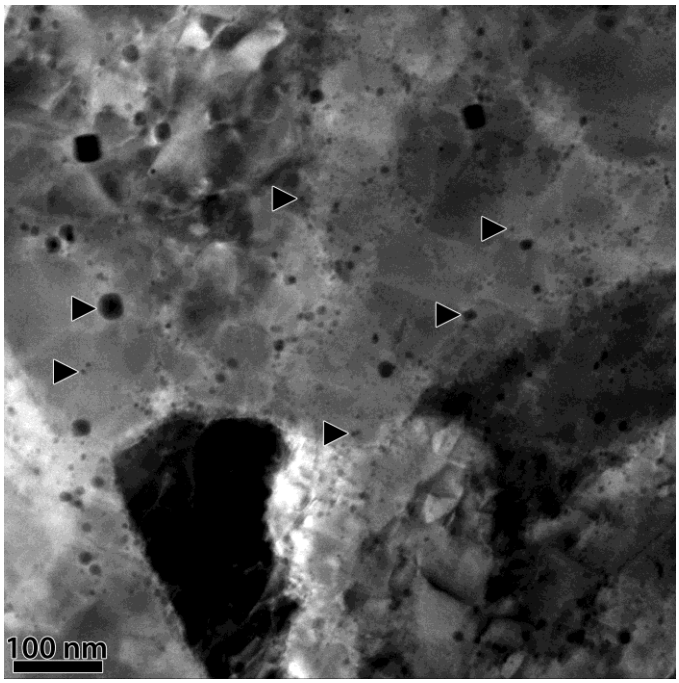

Fig. 4: HAADF STEM image of 14YWT material. Arrowheads mark oxide dispersion precipitates.

The MA956 alloy, shown in the HAADF image in Fig. 5(a), also has a uniform dispersion of oxide precipitates (appearing darker in the image). The oxides are larger than observed for 14YWT, with an average diameter of 14 nm and a standard deviation of 6.1 nm. Larger oxides were on the order of tens of nm. Composition of the oxides were observed to be rich in Y and Al compared to the surrounding matrix, as shown in the x-ray chemical maps presented in Fig. 5(b)-(e).

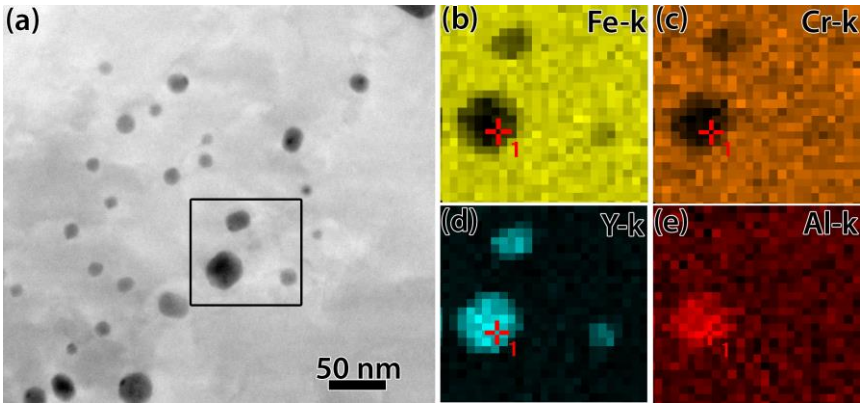

Fig. 5: (a) HAADF STEM image of MA956 and (b)-(e) x-ray chemical analysis of the region marked by the box. Precipitates appear to be rich in Y and Al.

Particle sizes are shown side by side for the two materials in Fig. 6. It is clear from the histograms that the particle size is smaller in the 14YWT material.

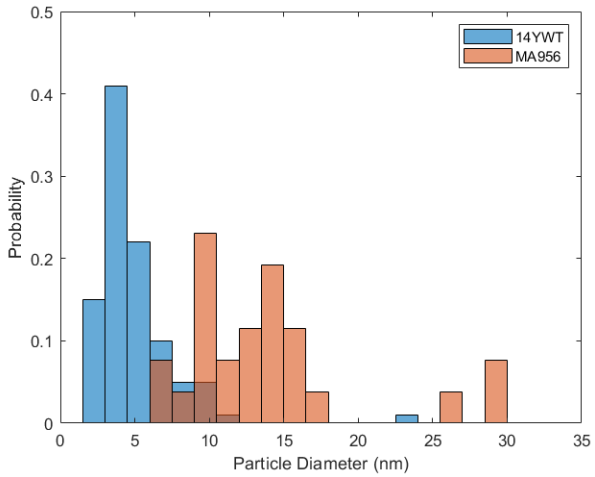

Figure 6: Histogram of particle size in both 14YWT and MA956.

4. Conclusions

Tubes of 14YWT and MA956 were characterized using EBSD orientation mapping and TEM. What was observed is a finer microstructure in the 14YWT which consisted of grains on the order of tens of µm and with dislocation content resulting in small crystallographic rotations within the grains. MA956, in contrast, was seen to have grains on the order of several hundred µm in the smallest dimension, though also with small crystallographic rotations within the grains. Oxide dispersion precipitate size was also smaller in the 14YWT, with the majority several nm in diameter, while precipitates in the MA956 were on the order of tens of nm.

5. References

[1] B.W. Baker, L.N. Brewer, Jom, 66 (2014) 2442-2457.